

The Gas-Phase Metallicity of Central and Satellite Galaxies in the SDSS

Anna Pasquali^{1*}, Anna Gallazzi² and Frank C. van den Bosch³

¹*Astronomisches Rechen-Institut, Zentrum für Astronomie der Universität Heidelberg, Mönchhofstrasse 12 - 14, 69120 Heidelberg, Germany*

²*Dark Cosmology Centre, Niels Bohr Institute, University of Copenhagen, Juliane Maries Vej 30, 2100 Copenhagen, Denmark*

³*Department of Astronomy, Yale University, P.O. Box 208101, New Haven, CT 06520-8101, USA*

ABSTRACT

We exploit the galaxy groups catalogue of Yang et al. and the galaxy properties measured in the SDSS Data Releases 4 and 7 to study how the gas-phase metallicities of star-forming galaxies depend on environment. We find that satellite and central galaxies follow a qualitatively similar stellar mass (M_*) - gas-phase metallicity relation, whereby their gas-phase metallicity increases with M_* . Satellites, though, have higher gas-phase metallicities than equally massive centrals, and this difference increases with decreasing stellar mass. We find a maximum offset of 0.06 dex at $\log(M_*/h^{-2}M_\odot) \simeq 8.25$. At fixed halo mass, centrals are more metal rich than satellites by ~ 0.5 dex on average. This is simply due to the fact that, by definition, centrals are the most massive galaxies in their groups, and the fact that gas-phase metallicity increases with stellar mass. More interestingly, we also find that the gas-phase metallicity of satellites increases with halo mass (M_h) at fixed stellar mass. This increment is more pronounced for less massive galaxies, and, at $M_* \simeq 10^9 h^{-2} M_\odot$, corresponds to ~ 0.15 dex across the range $11 < \log(M_h/h^{-1}M_\odot) < 14$. We also show that low mass satellite galaxies have higher gas-phase metallicities than central galaxies of the same stellar metallicity. This difference becomes negligible for more massive galaxies of roughly solar metallicity. We demonstrate that the observed differences in gas-phase metallicity between centrals and satellites at fixed M_* are not a consequence of stellar mass stripping (advocated by Pasquali et al. in order to explain similar differences but in stellar metallicity), nor to the past star formation history of these galaxies as quantified by their surface mass density or gas mass fraction. Rather, we argue that these trends probably originate from a combination of three environmental effects: (i) strangulation, which prevents satellite galaxies from accreting new, low metallicity gas which would otherwise dilute their ISM, (ii) ram-pressure stripping of the outer gas disk, thereby inhibiting radial inflows of low-metallicity gas, and (iii) external pressure provided by the hot gas of the host halo which prevents metal-enriched outflows from escaping the galaxies. Each of these three mechanisms naturally explains why the difference in gas-phase metallicity between centrals and satellites increases with decreasing stellar mass and with increasing host halo mass, at least qualitatively. However, more detailed simulations and observations are required in order to discriminate between these mechanisms, and to test, in detail, whether they are consistent with the data.

Key words: galaxies: abundances – galaxies: evolution – galaxies: fundamental parameters – galaxies: groups: general – galaxies: star formation

1 INTRODUCTION

Star forming galaxies in the local Universe define a fundamental plane, where their star formation rate (SFR) and gas-phase metallicity (typically $12 + \log(\text{O}/\text{H})$) correlate

with their stellar mass (M_* , cf. Lara-López et al. 2010; Mannucci et al. 2010). The individual relations in this plane have been long known; for example, Lequeux et al. (1979) were the first to recognize the existence of a correlation between galaxy magnitude and gas-phase metallicity, whereby more luminous galaxies exhibit higher metallicities. More observational evidence in support of such a dependence was

* E-mail: pasquali@ari.uni-heidelberg.de

later provided by Garnett & Shields (1987), Skillman et al. (1989) and Zaritsky et al. (1994) among others. The advent of the Sloan Digital Sky Survey (SDSS) made it possible for Tremonti et al. (2004) to transform the galaxy luminosity - metallicity relation into the more fundamental dependence of gas-phase metallicity on galaxy stellar mass, where the interstellar medium (ISM) of more massive galaxies is metal richer. Using the SDSS, Brinchmann et al. (2004) and Salim et al. (2005) established a correlation between the SFR of galaxies and their stellar mass, whereby more massive, star forming galaxies sustain larger star formation rates (see also Ellison et al. 2008). The star formation rate has been seen to correlate also with the gas-phase metallicity of galaxies, although in a way that differs according to the galaxy stellar mass. As pointed out by Mannucci et al. (2010), the gas-phase metallicity of low-mass galaxies decreases as their SFR increases, while high-mass galaxies do not show any significant dependence of their gas-phase metallicity on SFR (see also Yates et al. 2012).

Such an interplay among M_* , SFR and gas-phase metallicity of galaxies is usually explained in terms of stellar feedback triggering gas and metals outflows (see Edmunds 1990, Lehnert & Heckman 1996; Frye, Broadhurst & Benítez 2002; Garnett 2002; Tremonti et al. 2004; Kobayashi, Springel & White 2007; Scannapieco et al. 2008; Weiner et al. 2009; Spitoni et al. 2010; McCarthy et al. 2011; Peebles & Shankar 2011). Mannucci et al. (2010) envisaged a condition of steady-state in the local Universe, where infall of metal-poor gas (diluting the galaxy gas-phase metallicity and sustaining its star formation activity) occurs together with outflow of metal-rich gas whose efficiency should depend on the galaxy mass and SFR. Alternative explanations of the fundamental plane of star-forming galaxies invoke downsizing (where the star formation efficiency depends on galaxy mass, e.g. Brooks et al. 2007; Mouhcine et al. 2008; Calura et al. 2009), a dependence of the initial mass function on galaxy mass (Köppen, Weidner & Kroupa 2007) or a model of pure infall of metal-poor gas (Finlator & Davé 2008; Davé et al. 2010).

One can easily expect that environment may intervene in shaping the fundamental plane of star-forming galaxies. Environmental processes, such as strangulation (i.e. the removal of the gas reservoir of satellites after they are accreted by their host halo), ram pressure stripping (i.e. the removal of gas from satellites moving through a dense intra-cluster medium), galaxy harassment (i.e. high-speed impulsive galaxy encounters) and galactic wind confinement (i.e. due to the pressure exerted by the hot gaseous atmosphere of the host halo, which can inhibit galactic winds), are believed to alter the inflows/outflows of gas experienced by galaxies, modifying their star formation activity and their gas-phase metallicities with respect to that predicted by closed-box evolution.

Observations of the ISM in galaxies residing in the Lynx-Cancer void show that the gas-phase metallicity of these galaxies is lower by 30% on average than that of equally-massive galaxies in higher-density environments (Pustilnik, Tepliakova & Kniazev 2011).

Nearby clusters (such as Coma, Hercules and Virgo) have been extensively observed in search of environmental effects on the properties of star-forming galaxies. For example, Shields, Skillman & Kennicutt (1991) and

Skillman et al. (1996) found that the ISM of spiral galaxies in Virgo is on average metal-richer than that of comparable field galaxies. When a distinction is made on the basis of their HI content, the Virgo spirals that are HI deficient and also located closer to the cluster core are seen to have a higher gas-phase metallicity and a significantly lower birthrate (i.e. the ratio of newly-born stars to the stars formed in the past; Gavazzi et al. 2002) than those with normal HI content, which are usually located in the cluster outskirts and have similar metallicity as field galaxies. More recently, Petropoulou et al. (2011) have shown that spiral galaxies in the Hercules cluster are chemically evolved with an oxygen abundance close to solar, and their gas-phase metallicity does not depend on the local density within the cluster. Interestingly, their H α emission is less spatially extended than their optical disks and their star formation activity takes place preferentially in their inner regions. This result supports the picture where ram-pressure stripping due to the intergalactic medium (IGM) has truncated the HI disk of these spirals, with the result of preventing inflows of metal-poor gas from the outer disk and halo which would otherwise dilute the gas-phase metallicity in the inner regions of these galaxies. Suppression of infall of metal-poor gas due to environment would also be an explanation for the higher gas-phase metallicity of cluster spirals.

As for dwarf galaxies, the studies of Vílchez (1995) and Lee, McCall & Richer (2003) did not reveal a significant dependence of gas-phase metallicity on environment. On average, equally-bright dwarfs residing in the field and in Virgo do not differ in their O/H abundance, but some Virgo dwarfs can show a gas deficiency when compared with equally metal-rich dwarfs in the field. Such a gas deficiency seems to correlate with the X-ray surface brightness of the IGM, thus suggesting that ram-pressure stripping due to the IGM deprived these Virgo dwarfs of some of their gas. Ram-pressure stripping has been observed ‘in action’ for already a number of galaxies in Virgo (e.g. Crawl et al. 2010), whose HI disks appear distorted and truncated with respect to their stellar disks. A somewhat stronger dependence on environment was established by Petropoulou et al. (2011) for the dwarf galaxies in the Hercules cluster, whose gas-phase metallicity is seen increasing with local density. Metal-poorer dwarfs are associated with lower densities (typically the infall regions of the cluster) and with a stronger H α emission with respect to the global dwarf population in the cluster (Mahajan, Haines & Raychaudhury 2010), a sign that they undergo a starburst phase upon accretion onto the cluster. Such a star formation activity has to get quenched at later times in order to reproduce the observed fractions of red-and-dead satellites (e.g. van den Bosch et al. 2008; Kang & van den Bosch 2008; Kimm et al. 2009; Pasquali et al. 2009; Weinmann et al. 2009).

The large statistical power of the SDSS survey has not yet provided a definitive assessment of the environmental dependence of galaxy gas-phase metallicity. In Mouhcine, Baldry & Bamford (2007) the gas-phase metallicity – mass relation turns out to be weakly dependent on environment, defined as the number density of galaxies within the projected distance to the closest 4th and 5th neighbours. Star-forming galaxies show a marginal increase of their O/H abundance at fixed stellar mass in denser environments, equivalent to a few percent for the

Table 1. Samples statistics

	Description	Centrals	Satellites	Satellite Fraction
Sample <i>S</i>	galaxies with spectral S/N ≥ 20 and measured age and Z	70,067	13,626	19.4%
Sample <i>G</i>	galaxies with EW ($H\beta$) ≤ -3 Å and measured $12 + \log(O/H)$	69,688	14,182	20.4%
Sample <i>C</i>	galaxies that are both in Samples <i>S</i> and <i>G</i>	8,134	1,595	19.6%

more massive galaxies up to $\sim 20\%$ at $\log(M_*/M_\odot) < 9.5$. The authors concluded that the evolution of star forming galaxies is mainly driven by their intrinsic properties, and does not depend on environment at large. Cooper et al. (2008) found a stronger dependence of gas-phase metallicity on galaxy environment (defined as the number density of galaxies within the projected distance to the closest 3rd neighbour), in that galaxies residing in higher density environments are metal-richer (see also Ellison et al. 2009). The question arises whether these differences between Mouhcine, Baldry & Bamford (2007) and Cooper et al. (2008) may be due to different definitions of environment. As already discussed by e.g. Weinmann et al. (2006) and recently Muldrew et al. (2011), the projected number density of galaxies is of ‘tricky’ interpretation as it depends on environment itself. In massive haloes such as clusters, it probes environment on a scale smaller than the halo virial radius, while in low mass haloes the environment probed typically encompasses multiple dark matter haloes.

In this paper, we revisit the issue of gas-phase metallicity vs. galaxy environment by making use of the catalogue of galaxy groups extracted from the SDSS Data Release 4 by Yang et al. (2007). In this catalogue, environment is defined as the total amount of dark matter associated with each galaxy group, and also allows us to distinguish (and treat separately) central from satellite galaxies, for which semi-analytic models of galaxy formation and evolution predict rather different evolutionary paths. We aim at achieving a detailed assessment of how gas-phase metallicities of galaxies depend on galaxy stellar mass (over the interval $8 < \log(M_*/h^{-2}M_\odot) < 11$), hierarchy (centrals vs satellites) and environment across a large range of halo masses ($11 < \log(M_h/h^{-1}M_\odot) < 14$), in order to gain important insights into how environment regulates gas inflows feeding the star formation activity of galaxies, and affects the efficiency of galactic outflows through the pressure applied by the intra-group hot gas.

This paper is organized as follows. In Sect. 2 we describe the catalogue of galaxy groups obtained by Yang et al. (2007) for the SDSS Data Release 4 (DR4). The stellar mass - gas-phase metallicity relation obtained for satellites and centrals separately is discussed in Sect. 3, while the halo mass - gas-phase metallicity relation is presented in Sect. 4. The results are discussed in Sect. 5 and the conclusions follow in Sect. 6. Throughout this paper we adopt a flat Λ CDM cosmology with $\Omega_m = 0.238$ and $\Omega_\Lambda = 0.762$ (Spergel et al. 2007) and we express units that depend on the Hubble constant in terms of $h = H_0/(100 \text{ km s}^{-1} \text{ Mpc}^{-1})$.

2 DATA

Our analysis is based on the SDSS DR4 catalogue of galaxy groups constructed by Yang et al. (2007) by applying the halo-based group finder algorithm of Yang et al. (2005) to the New York University Value-Added Galaxy Catalogue (NYU-VAGC, Blanton et al. 2005) extracted from SDSS DR4 (Adelman-McCarthy et al. 2006). From the NYU-VAGC Main Galaxy Sample Yang et al. (2007) selected all galaxies with an apparent magnitude (corrected for Galactic foreground extinction) brighter than $r = 18$ mag, in the redshift range $0.01 \leq z \leq 0.20$ and with a redshift completeness $C_z > 0.7$. These galaxies were used to build three galaxy groups samples: sample I, which only uses the 362356 galaxies with measured redshifts from the SDSS; sample II, which includes an additional 7091 galaxies with SDSS photometry but redshifts taken from alternative surveys; sample III which lists an additional 38672 galaxies lacking a redshift due to fibre collisions, but being assigned the redshift of their nearest neighbour (cf. Zehavi et al. 2002). This paper focuses solely on sample II, where galaxies are split into ‘centrals’ (defined as the most massive group members on the basis of their M_*) and ‘satellites’ (all group members that are not centrals). Galaxy magnitudes and colours are based on the standard SDSS Petrosian technique (Petrosian 1976; Strauss et al. 2002), are corrected for Galactic foreground extinction (Schlegel, Finkbeiner & Davis 1998) and K -corrected and evolution corrected to $z = 0.1$ according to the procedure of Blanton et al. (2003). We use the notation $^{0.1}M_X$ to indicate the resulting absolute magnitude in the photometric X band. Galaxy stellar masses are computed using the relation between stellar mass-to-light ratio and colour of Bell et al. (2003), and galaxy morphology is defined in terms of the concentration parameter ($C = r_{90}/r_{50}$ where r_{90} and r_{50} are the radii encompassing 90% and 50% of the Petrosian r -band flux, respectively). Values of C larger than 2.6 typically refer to bulge-dominated galaxies (cf. Strateva et al. 2001).

For each group in the catalogue Yang et al. (2007) provided two estimates of its dark matter halo mass, M_h , one based on the ranking of its total luminosity, the other on the ranking of its total stellar mass. These halo masses deviate from each other by about 0.1 dex at low M_h and 0.05 dex at the massive end. The method of Yang et al. (2007) is able to assign M_h only to groups more massive than $\sim 10^{12} h^{-1} M_\odot$ and with one or more members brighter than $^{0.1}M_r - 5 \log h = -19.5$ mag. For all the other groups, Yang, Mo & van den Bosch (2008) used the relations between the luminosity (or M_*) of central galaxies and the halo mass of their groups to estimate the halo mass of single central galaxies down to $M_h \sim 10^{11} h^{-1} M_\odot$. In what follows we will use the halo masses derived from the group’s total stellar mass, because, as shown by More et al. (2011), stellar mass is a better indicator of halo mass than luminos-

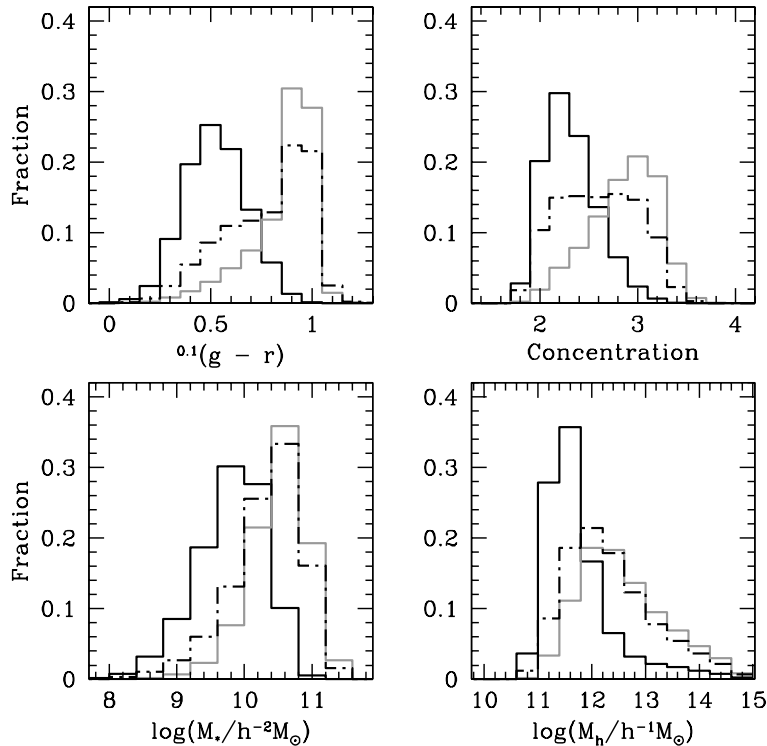


Figure 1. The normalized distributions of sample II (black dot-dashed line) and samples *S* and *G* (solid grey and black, respectively) in colour, concentration, stellar mass and halo mass. The distributions are not weighted by $1/V_{\max}$.

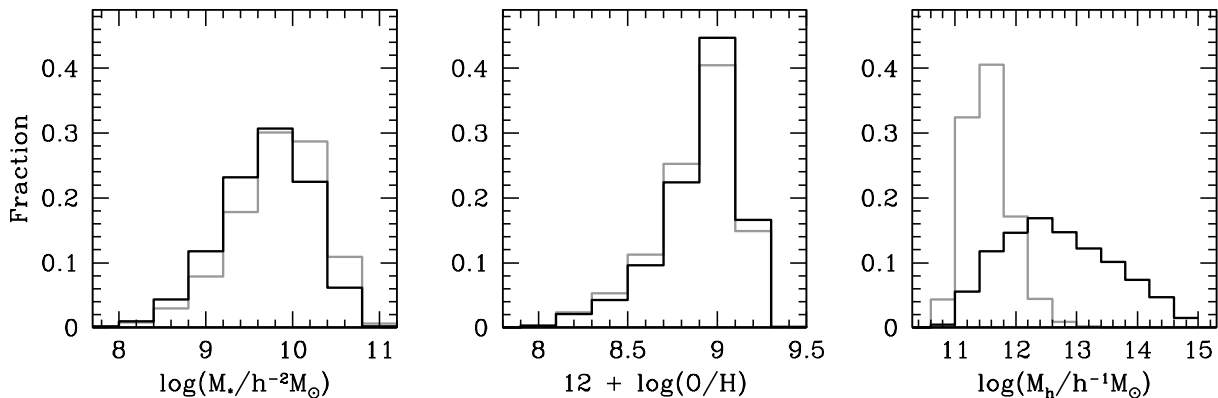


Figure 2. The normalized distributions of centrals (grey) and satellites (black) in sample *G* in stellar mass, gas-phase metallicity and halo mass. The distributions are not weighted by $1/V_{\max}$.

ity. Since the groups catalogue of Yang et al. (2007) is not volume limited, it suffers from the Malmquist bias, which causes an artificial increase of the average luminosity (and M_*) of galaxies with increasing redshift. This effect is especially important for satellites, since they span a large range of stellar masses within each halo. We take the Malmquist bias into account by weighting each galaxy by $1/V_{\max}$, where V_{\max} is the comoving volume of the Universe out to a comoving distance at which a galaxy would still have made the selection criteria of the groups sample. Therefore, all distributions in the following sections are weighted by $1/V_{\max}$ unless specified otherwise.

2.1 Stellar population parameters: sample *S*

We matched sample II with the catalogue of stellar ages and metallicities obtained by Gallazzi et al. (2005) for the galaxies in the SDSS DR4. Briefly, Gallazzi et al. (2005) compared the strength of stellar absorptions in the observed spectrum of each galaxy with the predictions of a Monte Carlo library of 150 000 star formation histories (SFHs), based on the Bruzual & Charlot (2003) population synthesis code and the Chabrier (2003) initial mass function. The SFHs in the library have a declining star formation rate (SFR) over varying timescales, and are superposed with random bursts of varying intensity and duration. These bursts are added in such a way that only 10% of the models can experience a burst of star formation in the last 2 Gyr. For each

galaxy a probability density distribution of stellar r -band flux-weighted stellar ages and metallicities can be derived, whose median values we will use for our analysis below. It has to be noted that the stellar ages and metallicities derived as above refer to the redshift at which galaxies are observed. No correction to $z = 0$ was attempted because this would require an accurate knowledge of the SFH from the redshift of the observations to the present. The uncertainty on the stellar ages and metallicities depends on the spectral signal-to-noise (S/N); a $S/N \geq 20$ ensures $\Delta \log(Z) < 0.3$ dex, $\Delta \log(\text{Age}) < 0.2$ dex and an average uncertainty on both parameters of ~ 0.12 dex.

All galaxies in sample II which have a spectral $S/N \geq 20$ and a stellar age and metallicity estimates computed as in Gallazzi et al. (2005) hereafter constitute our sample S . This sample was extensively studied by Pasquali et al. (2010), who found that satellites are older and metal richer than centrals of the same M_* , and this difference increases with decreasing M_* . In addition, the average age and stellar metallicity of low-mass satellites ($M_* \leq 10^{10} h^{-2} M_\odot$) increase with the mass of the halo in which they reside. The authors interpreted these trends as due to the quenching of star formation in satellites, which leaves their stellar populations to evolve passively (thus explaining their older ages), and to tidal stripping, which removes a non-negligible fraction of their stellar mass. In this picture, the stellar metallicity of present-day satellites reflects the maximum stellar mass that they reached during their lifetime and which can be significantly higher than their present-day M_* .

2.2 Gas metallicities and star formation rates: sample G

Sample II was also cross-matched with the catalogue of gas-phase metallicities [i.e. $12 + \log(\text{O}/\text{H})$] published by Tremonti et al. (2004) for the galaxies in SDSS DR4. The analysis performed by Tremonti et al. (2004) can briefly be summarized in the following steps: *i*) the continuum emission in each galaxy spectrum was modelled with a combination of single stellar populations from Bruzual & Charlot (2003) of the same stellar metallicity, also convolved with the extinction law of Charlot & Fall (2000), and subsequently subtracted from the observed spectrum. *ii*) The lines in the resulting pure emission-lines spectrum were simultaneously fitted with Gaussians by imposing that all the Balmer lines have the same width and velocity offset, and likewise for the forbidden lines. *iii*) The gas-phase metallicity was statistically estimated for all star forming galaxies by fitting the more prominent emission lines with the models of Charlot & Longhetti (2001). These models combine the synthetic stellar populations of Bruzual & Charlot (2003) with the photoionization code CLOUDY (Ferland 1996) and the Charlot & Fall (2000) extinction law, so that the galaxy ISM conditions (e.g. gas ionization, metallicity and dust attenuation) are intertwined with the radiation field and nuclear synthesis of the underlying stellar populations. For each galaxy Tremonti et al. (2004) derived a likelihood distribution of the gas-phase metallicity from which we extracted the median, the 16th and 84th percentile values. All galaxies in sample II whose $\text{H}\beta$ equivalent width is $\text{EW}(\text{H}\beta) \leq -3 \text{ \AA}$ (corresponding to a $S/N \geq 10$) and whose gas-phase

metallicity is available from Tremonti et al. (2004) make up our sample G .

For the galaxies in sample G we retrieved the median values of stellar mass, m_{fib} , star formation rate, SFR_{fib} , and specific SFR_{fib} ($\text{sSFR}_{\text{fib}} = \text{SFR}_{\text{fib}}/m_{\text{fib}}$) in the fibre, the median values of global star formation rate, SFR_{glo} , and specific SFR_{glo} ($\text{sSFR}_{\text{glo}} = \text{SFR}_{\text{glo}}/M_*$) from the SDSS Data Release 7. For star forming galaxies (like those in sample G), the SFR_{fib} was directly computed from their emission lines following the procedure of Brinchmann et al. (2004), who modelled the observed emission lines with the models of Charlot & Longhetti (2001). The global star formation rate of the galaxies in DR7 was derived by fitting the photometry of the outer regions of galaxies with the synthetic stellar population models of Bruzual & Charlot (2003) convolved with the extinction law of Charlot & Fall (2000) (cf. Salim et al. 2007). Using this same procedure, Brinchmann et al. (2004) derived the global and fibre stellar masses, M_* and m_{fib} , from the galaxy integrated magnitudes and the magnitudes measured within the fibre.

2.3 Combined sample

We extracted from sample G all galaxies for which the spectral S/N is larger than 20, and the stellar age and metallicity are available together with their gas-phase metallicity and star formation rate. We refer to this subset of objects as the composite sample, i.e. sample C . Table 1 summarizes the number of central and satellite galaxies in the samples S , G and C defined above. In Fig. 1 we compare the normalized distributions of the galaxies in sample II (black dashed line), sample S (grey solid line) and G (black solid line) in colour, concentration, stellar and halo masses. We note that the sample definition introduces a clear separation in colour and concentration between sample G and sample S . Being star forming, the galaxies in sample G turn out to be bluer and more disk-like (with lower concentrations) than those in sample S . As already shown by Pasquali et al. (2009), star forming galaxies have on average lower M_* and preferentially reside in low-mass haloes. This trend is mainly due to the central galaxies of sample G as it can be inferred from the right-hand panel of Fig. 2, while the satellites in the same sample span a wide range of environments from $M_h \simeq 10^{11}$ to $10^{15} h^{-1} M_\odot$. In addition, centrals seem to be slightly more massive and metal-poorer than satellites in sample G (left-hand and middle panels of Fig. 2). It is also interesting to compare sample S and sample C in stellar age and metallicity; we find in Fig. 3 that the star forming galaxies in sample C have on average younger and metal-poorer stellar populations than those in sample S . We are thus probing different ranges of galaxy properties with respect to the analysis in Pasquali et al. (2010).

3 THE STELLAR MASS - GAS-PHASE METALLICITY RELATION

The dependence of gas-phase metallicity on stellar mass is plotted in Fig. 4 for centrals (grey) and satellites (black). We computed the median (solid lines), the 16th and 84th percentile values (dashed lines) of the gas-phase metallicity distribution of centrals and satellites in sample G per bin of

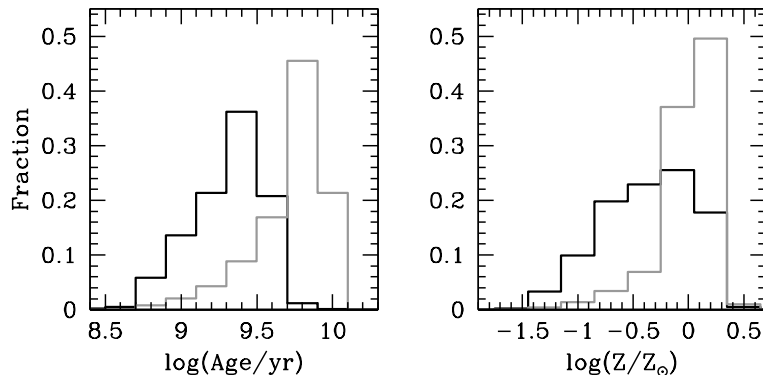


Figure 3. The normalized distributions of galaxies in sample *S* (grey) and sample *C* (black) in stellar age and metallicity. The distributions are not weighted by $1/V_{\max}$.

M_* . It turns out that centrals and satellites follow a qualitatively similar relation between gas-phase metallicity and M_* , whereby the metallicity of their gas increases with their stellar mass. The gas in satellites is, though, metal richer than in centrals at nearly all stellar masses, and this is true for the median values as well as for the 16th and 84th percentiles.

The difference in the median $12 + \log(\text{O}/\text{H})$ between satellites and centrals decreases from 0.06 dex at $\log(M_*/h^{-2}M_\odot) \simeq 8.25$ to 0.004 dex at $\log(M_*/h^{-2}M_\odot) \simeq 10.75$. This trend holds also for volume limited sub-samples extracted from sample *G*.

For each bin of stellar mass, we constructed the cumulative distributions in $12 + \log(\text{O}/\text{H})$ of centrals and satellites, and used the Kolmogorov - Smirnov (KS), two sample test to assess the statistical significance of the metallicity offset seen in Fig. 4. The probability at which the null hypothesis (i.e. centrals and satellites are drawn from the same population) is rejected is larger than 95% in the range $8 \leq \log(M_*/h^{-2}M_\odot) \leq 10.5$, and drops to $\sim 19\%$ for galaxies more massive than $M_* = 10^{10.5} h^{-2}M_\odot$. Thus, over the stellar mass range spanned by our sample, the cumulative distributions indicate that satellites have a higher gas-phase metallicity than centrals.

In order to check whether/how the M_* - gas-phase metallicity relation of satellites depends on environment, we derived it for satellites split among different bins of halo mass. The results are shown in Fig. 5, where satellites residing in different groups are colour coded; the black dashed line traces the median $12 + \log(\text{O}/\text{H})$ of centrals from Fig. 4 and the grey band represents the 16th - 84th percentile range of the distribution of centrals also from Fig. 4. The 1σ errorbars represent the error on the mean gas-phase metallicity weighted by $1/V_{\max}$, and were computed by propagating the uncertainties associated with the individual measurements of $12 + \log(\text{O}/\text{H})$. Satellites less massive than $\log(M_*/h^{-2}M_\odot) \simeq 9.3$ and in groups more massive than $\log(M_h/h^{-1}M_\odot) \simeq 12$ appear to follow the same M_* - gas-phase metallicity relation. The overall shift to higher gas-phase metallicities of satellites with respect to centrals is due only to satellites in haloes more massive than $10^{12} h^{-1}M_\odot$, with their stellar mass - gas-phase metallicity relation slightly steepening as M_h increases.

Satellites in the least massive groups ($11 < \log(M_h/h^{-1}M_\odot) < 12$) and more massive than

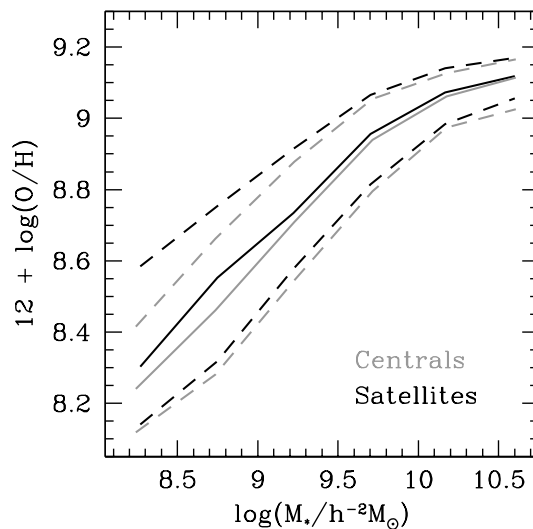


Figure 4. The M_* - gas-phase metallicity relation for central (grey) and satellite (black) galaxies. The solid lines represent the median metallicity, while the dashed lines the 16th and 84th percentiles of the metallicity distribution of centrals and satellites in each bin of stellar mass. Centrals and satellites belong to sample *G*.

$\log(M_*/h^{-2}M_\odot) = 9.3$ are very similar to centrals in terms of their gas-phase metallicity, while less massive satellites exhibit higher $12 + \log(\text{O}/\text{H})$ values than centrals as their stellar mass decreases [the maximum difference, $+0.11$ dex, is registered at $\log(M_*/h^{-2}M_\odot) \simeq 8.2$].

4 THE HALO MASS - GAS-PHASE METALLICITY RELATION

We show in Fig. 6 the dependence of the gas-phase metallicity of central and satellite galaxies on the halo mass of the group in which they reside. The grey and black lines refer to centrals and satellites, respectively; the solid and dashed lines represent the 50th and 16th/84th percentiles of the gas-phase metallicity distribution within each bin of M_h . In halos with $M_h \lesssim 10^{12} h^{-1}M_\odot$ the gas-phase metallicity of central galaxies increases sharply with halo mass. Centrals in more massive halos, though, have roughly constant

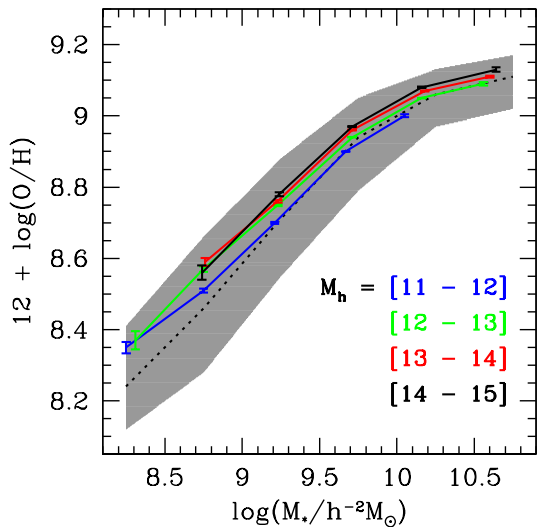


Figure 5. The M_* - gas-phase metallicity relation for centrals (grey) and satellites (colour) split among different bins of halo mass. The black dashed line represents the median $12 + \log(\text{O}/\text{H})$ of centrals, while the grey band marks the 16th - 84th percentile range of the distribution of centrals.

gas-phase metallicities. Note that the small number statistics for massive groups in the Yang et al. (2007) catalogue prevent us from probing this halo mass dependence beyond $M_h \sim 10^{14} h^{-1} M_\odot$. Regardless of halo mass, central galaxies are metal richer than satellites in halos of the same mass by ~ 0.5 dex on average. This is simply a reflection of the fact that, by definition, central galaxies are the more massive galaxies in their groups, combined with the fact that gas-phase metallicity is an increasing function of stellar mass. The oxygen abundance of satellites smoothly increases with halo mass up to $M_h \simeq 10^{13} h^{-1} M_\odot$, and is constant in more massive groups. Overall, it is seen increasing by ~ 0.5 dex across the full range of environments probed by sample G , in agreement with the findings of Cooper et al. (2008).

We split the satellites in sample G among different bins of stellar mass and computed their M_h - gas-phase metallicity relation as a function of M_* . The results are illustrated in the left hand panel of Fig. 7, where satellites are colour coded on the basis of their stellar mass. The black dashed line traces the median $12 + \log(\text{O}/\text{H})$ of centrals as a function of M_h (from Fig. 6), while the grey band indicates their 16th-to-84th percentile distribution in gas-phase metallicity as shown in Fig. 6. The 1σ errorbars for satellites represent the error on the mean gas-phase metallicity weighted by $1/V_{\text{max}}$, and were computed by propagating the uncertainties associated with the individual measurements of $12 + \log(\text{O}/\text{H})$. The offset in $12 + \log(\text{O}/\text{H})$ among the different M_h - gas-phase metallicity relations is simply due to stellar mass. We see that the gas-phase metallicity of satellites increases with their halo mass in all bins of M_* . The amplitude of this trend across the full M_h range amounts to ~ 0.15 dex for satellites with $\log(M_*/h^{-2} M_\odot) < 9$, ~ 0.1 dex for those with $9 < \log(M_*/h^{-2} M_\odot) < 10.5$ and only ~ 0.02 dex for the most massive satellites. These findings are consistent with the results of Mouhcine, Baldry & Bamford (2007). To better illustrate the dependence of gas-phase metallicity on M_h , we computed the slope $d[12 + \log(\text{O}/\text{H})]/d[\log(M_h)]$ in

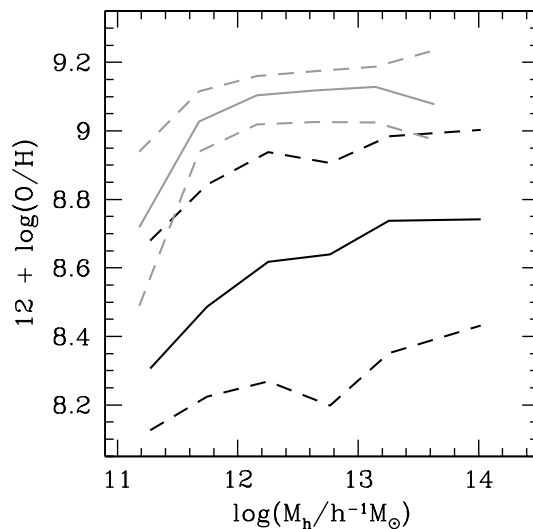


Figure 6. The M_h - gas-phase metallicity relation for central (grey) and satellite (black) galaxies. The solid lines represent the median metallicity, while the dashed lines the 16th and 84th percentiles of the metallicity distribution of centrals and satellites in each bin of stellar mass. Centrals and satellites belong to sample G .

each stellar mass bin, and plotted it as a function of M_* in the right hand panel of Fig. 7. A weak trend can be recognized whereby the strength of the M_h - gas-phase metallicity relation decreases with increasing stellar mass.

5 DISCUSSION

In the previous sections we have shown that the gas-phase metallicity of central and satellite galaxies depends primarily on their stellar mass. In agreement with the results of Tremonti et al. (2004), their gas becomes metal richer as their stellar mass increases. However, at fixed M_* the gas-phase metallicity is higher in satellites than in centrals, and this observed offset increases with decreasing stellar mass. In addition, at fixed M_* the oxygen abundance of satellites is found to be higher in more massive haloes. This trend is observed for satellites less massive than $M_* \simeq 10^{10.5} h^{-2} M_\odot$ with an amplitude of ~ 0.1 dex over the range $11 < \log(M_h/h^{-1} M_\odot) < 14$, and becomes considerably weaker for the most massive satellites. Hence, there is a clear and ‘pure’ dependence of the gas-phase metallicity of satellites on environment, but this dependence is much weaker than the dependence on stellar mass. In what follows we investigate the physical mechanisms that may be responsible for the (M_*, M_h) - gas-phase metallicity relations of satellite galaxies.

5.1 Gas-phase and stellar metallicities

We start by comparing the properties in common between the galaxies in sample C and those in sample S . We recall that sample C is built from sample S and includes only galaxies with gas-phase metallicity, stellar age and metallicity, while sample S contains galaxies with measured stellar age and metallicity, regardless of whether their gas-phase

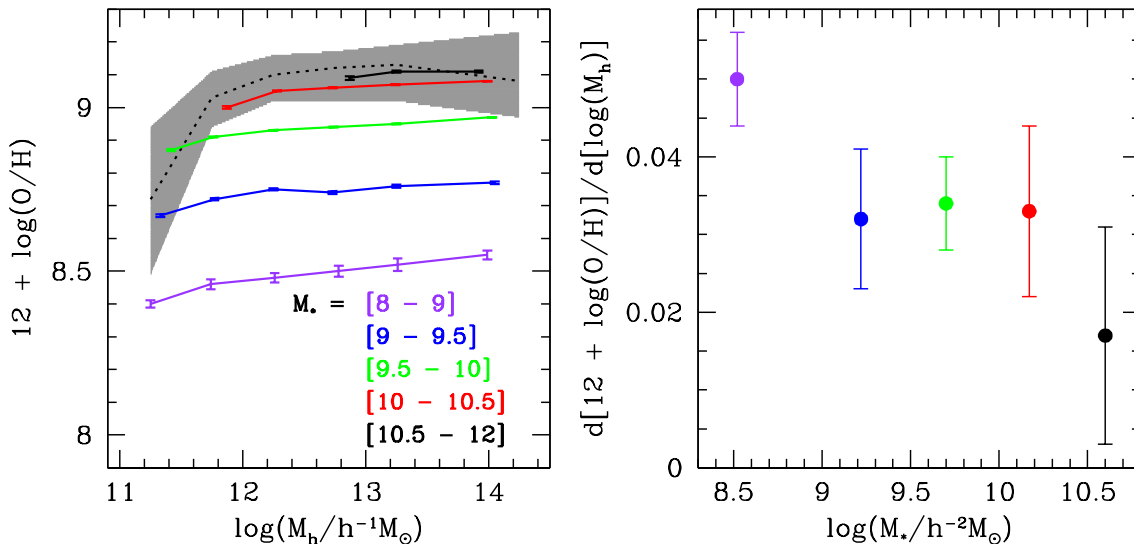


Figure 7. *Left:* the M_h - gas-phase metallicity relation for satellite galaxies (colour) split among different bins of stellar mass. The black dashed line represents the median metallicity of centrals, while the grey band shows the 16th - 84th percentiles distribution of centrals as a function of halo mass. Centrals and satellites belong to sample *G*. *Right:* the slope of the M_h - gas-phase metallicity relations shown in the left hand panel is plotted as a function of stellar mass. The errorbars indicate the 1σ uncertainty.

metallicity is available (see Sect. 2). Similarly to sample *G* (cf. Fig. 4), also the satellites in sample *C* display a higher median oxygen abundance when compared with equally massive centrals. Figure 8 shows that their difference in median $12 + \log(\text{O}/\text{H})$ at fixed M_* decreases from ~ 0.14 dex at $M_* < 10^9 h^{-2} M_\odot$ to ~ 0.02 dex at $M_* < 10^{10.3} h^{-2} M_\odot$. Note that this difference is larger than that measured between centrals and satellites in sample *G* as shown in Fig. 4. This is likely to be a consequence of the fact that sample *C* is biased towards galaxies with weaker emission lines and lower star formation activity than those in sample *G*. In this respect, satellites in sample *C* may have been more significantly quenched by their environment than satellites in sample *G*. We caution, though, that sample *C* suffers from small number statistics when compared to sample *G*. The KS two sample test performed on the cumulative distributions in $12 + \log(\text{O}/\text{H})$ of centrals and satellites in sample *C* in different bins of stellar mass establishes that satellites are metal richer than centrals at a confidence level between 78% and 100% in the range $8 < \log(M_*/h^{-2}M_\odot) < 10.5$, while the most massive satellites can not be distinguished from equally massive centrals.

Using sample *S*, Pasquali et al. (2010) found that satellites have older, luminosity-weighted ages and higher stellar metallicities than equally massive centrals. Both these differences become smaller for more massive galaxies. In addition, they showed that satellites with $M_* \lesssim 10^{10} h^{-2} M_\odot$ have ages and metallicities that increase with the mass of the host halo in which they reside. Pasquali et al. (2010) explained these trends by invoking *i*) strangulation, i.e. the removal of the gas reservoir of satellites after they are accreted by their host halo. The consequent quenching of star formation leaves the stellar populations of satellites to evolve passively, while the more prolonged star formation activity of centrals keeps their luminosity-weighted age younger. *ii*) Tidal stripping, which causes satellites to lose stellar mass once they have been accreted onto their host group. The fact that present

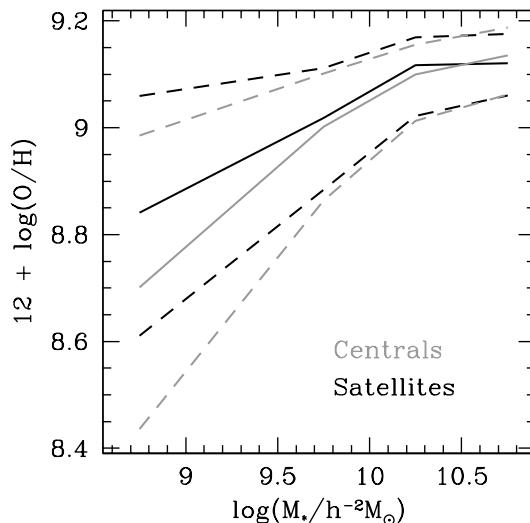


Figure 8. The M_* - gas-phase metallicity relation for central (grey) and satellite (black) galaxies in sample *C*, i.e. with measures of both gas and stellar metallicity. The solid lines represent the median metallicity, while the dashed lines represent the 16th and 84th percentiles of the metallicity distribution of centrals and satellites in each bin of stellar mass.

day satellites descend from more massive progenitors is left imprinted in their stellar metallicity, which is not expected to change significantly after a satellite is accreted onto a bigger halo and its star formation activity is quenched. The effects of strangulation and tidal stripping likely depend on the time of infall, i.e. when a galaxy became a satellite for the first time. The earlier the infall time is, the older and less massive a satellite is, and the more massive the group in which the satellite resides (given that more massive haloes assemble earlier). This dependence on infall time naturally explains why the ages and stellar metallicities of satellites increase with M_h .

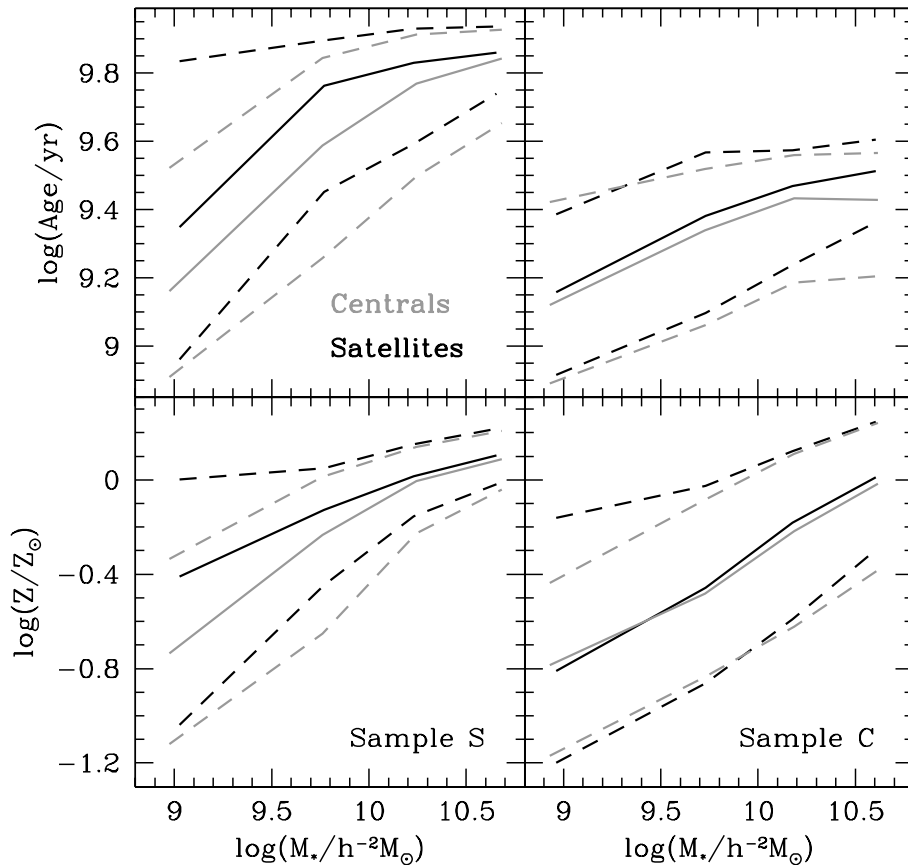


Figure 9. The distributions of stellar age and metallicity as a function of stellar mass for centrals (grey) and satellites (black) belonging to sample *S* (left hand panels) and to sample *C* (right hand panels). The solid lines represent the median age/metallicity, while the dashed lines the 16th and 84th percentiles of the age/metallicity distribution of centrals and satellites in each bin of stellar mass.

Since both stellar and gas-phase metallicities correlate with M_* , one might also expect the higher gas-phase metallicities of satellites (with respect to centrals of the same M_*) to be a manifestation of tidal stripping. In this scenario, satellites have higher gas-phase metallicities than centrals of the same *present-day* mass, simply because they had a higher stellar mass at infall: the gas-phase metallicity serves as an indicator of the maximum stellar mass the galaxy reached during its lifetime. In order to test this hypothesis, we compare in Fig. 9 the M_* - stellar age and the M_* - stellar metallicity relations of centrals and satellites in sample *S* with those of centrals and satellites in sample *C*. As already pointed out by Fig. 3, the galaxies in sample *C* are characterized by younger stellar ages and lower stellar metallicities than those in sample *S*. At fixed stellar mass satellites are systematically older than centrals in both samples. This age difference is rather small for sample *C* (about 0.04 dex at $M_* < 10^{10} h^{-2} M_\odot$), and statistically significant only for galaxies more massive than $10^{9.5} h^{-2} M_\odot$. In fact, the KS two sample test applied to the age cumulative distributions of sample *C* indicates that centrals and satellites with $\log(M_*/h^{-2}M_\odot) > 9.5$ are drawn from two different populations at a $>92\%$ confidence level, while less massive centrals and satellites belong to the same parent population. In sample *S* the age difference between satellites and centrals is larger, and decreases from 0.19 dex at $M_* < 10^9 h^{-2} M_\odot$ to 0.02 dex at $M_* < 10^{10.5} h^{-2} M_\odot$. The

KS two sample test applied to the age cumulative distributions of centrals and satellites in different M_* bins shows that the hypothesis of centrals and satellites belonging to the same population is rejected at a $>99\%$ confidence level. We may thus conclude that the satellites in sample *C* were accreted later and their star formation activity has been quenched less than the satellites in sample *S*. Consequently, they should have also experienced less tidal stripping, so that their stellar metallicities should be closer to those of equally massive centrals. This is indeed the case; the bottom panels of Fig. 9 show that satellites in sample *C* have stellar metallicities that are basically indistinguishable from those of centrals of the same stellar mass. The differences are less than 0.02 dex, implying that satellites in sample *C* have lost $<10\%$ of their pre-infall stellar mass. For comparison, the difference in the median $\log(Z/Z_\odot)$ between satellites and centrals in sample *S* decreases from ~ 0.3 dex at $M_* < 10^9 h^{-2} M_\odot$ to <0.02 dex at $M_* > 10^{10} h^{-2} M_\odot$, indicating that satellites in sample *S* have lost between $\sim 75\%$ (for a present day $M_* = 10^9 h^{-2} M_\odot$) and $\sim 20\%$ (for a present day $M_* = 10^{10.5} h^{-2} M_\odot$) of their stellar mass at infall. To summarize, Fig. 9 indicates that satellites in sample *C* have not suffered significant tidal stripping (yet), but have undergone quenching of their star formation activity at some, small degree. Therefore, we conclude that stellar mass stripping cannot explain why satellites have higher gas-phase metallicities than centrals of the same stellar mass.

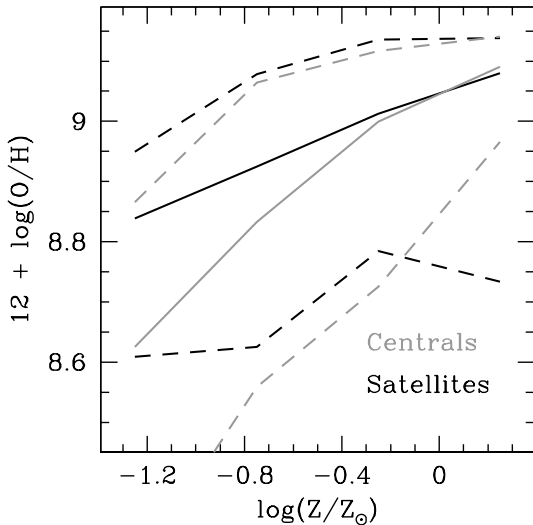


Figure 10. The dependence of the gas-phase metallicity of centrals (grey) and satellites (black) in sample *C* on their stellar metallicity. The solid lines trace the median $12 + \log(\text{O}/\text{H})$, while the dashed lines the 16th and 84th percentiles of the gas-phase metallicity in each bin of stellar metallicity.

In further support of this conclusion, we directly compare the gas-phase metallicities of centrals and satellites at fixed stellar metallicity in Fig. 10. If the same stellar stripping responsible for creating the (small) offset in stellar metallicity between star-forming centrals and satellites were the only responsible for the observed offset in gas-phase metallicities, we would expect the relation between gas-phase and stellar metallicity to be the same for central and satellite galaxies. Figure 10 shows that clearly this is not the case: at $\log(Z/Z_{\odot}) < -0.4$ (corresponding to $M_{\star} < 10^{9.5} h^{-2} M_{\odot}$, see Fig. 9) satellites have higher gas-phase metallicities than centrals of the same stellar metallicity. Rather, Fig. 10 suggests that the differences in gas-phase metallicity between centrals and satellites have their origin in something that is specific to the gas and that has a larger impact on less chemically evolved (hence preferentially low-mass) galaxies. The scatter between gas-phase and stellar metallicity has been shown to be associated with variations in stellar surface mass density, star formation rate and gas mass fraction (Gallazzi et al. 2005). In the next sections we test whether any of these parameters may indeed be associated with the difference in gas-phase metallicity between centrals and satellites.

5.2 Surface mass densities

Kauffmann et al. (2003) have shown that the star formation activity of low mass galaxies depends more on their surface mass density than on their stellar mass. In a naive closed-box model for chemical evolution, this would imply that, at fixed M_{\star} , galaxies with a higher surface mass density have transformed a larger amount of gas into stars and hence increased their gas-phase metallicity. For the galaxies in sample *G* we define the surface mass density in the fibre as $\Sigma_{\text{fib}} = m_{\text{fib}}/\text{area}_{\text{fib}}$, where area_{fib} is the physical area covered by the SDSS fibre ($3''$ in diameter) at the galaxy distance. We use Σ_{fib} as a proxy for the past star formation

history that took place over the same (central) regions from which the gas-phase metallicities have been measured. The solid lines in the left hand panel of Fig. 11 plots the median Σ_{fib} of centrals (grey) and satellites (black) as a function of their stellar mass; the dashed lines indicate the corresponding 16th and 84th percentiles. The difference in Σ_{fib} between satellites and centrals is ~ 0.02 dex at most, and changes from being negative at $\log(M_{\star}/h^{-2}M_{\odot}) < 9.5$ (Σ_{fib} is lower in satellites) to positive at higher M_{\star} . In the right hand panel of Fig. 11 the median oxygen abundance (solid line) of centrals (grey) and satellites (black) is shown as a function of their surface mass density; as expected from the findings of Kauffmann et al. (2003), the gas-phase metallicity increases with Σ_{fib} for both centrals and satellites. When matched in Σ_{fib} , satellites with $\log(\Sigma_{\text{fib}}) < 8.5$ display a higher gas-phase metallicity than centrals in the median and 16th and 84th percentiles values. We therefore conclude that the offsets in $12 + \log(\text{O}/\text{H})$ are not associated with any offsets in surface mass density, as expected in a simple closed box model if the different gas-phase metallicities of centrals and satellites owe to differences in their star formation histories.

5.3 Gas mass fractions

Similarly to Σ_{fib} , the gas mass fraction can be considered an indirect measurement of the past star formation activity undergone by galaxies. It has been shown by Zhang et al. (2009) that the HI gas mass fraction of galaxies decreases along the gas-phase metallicity - stellar mass relation as both M_{\star} and the oxygen abundance increase. Moreover, at fixed stellar mass, gas - poor galaxies exhibit higher gas-phase metallicities. This poses the question whether the difference in gas-phase metallicity between central and satellite galaxies reflects a difference in their gas mass fractions. In order to test this, we computed the gas mass fraction in the fibre for central and satellite galaxies using Eq. (5) of Tremonti et al. (2004); i.e., we derive the surface gas mass density, Σ_{gas} , from the star formation surface density in the fibre by inverting the Schmidt law given by Kennicutt (1998). The gas mass fraction in the fibre is then defined as $\mu_{\text{gas}} = \Sigma_{\text{gas}}/(\Sigma_{\text{gas}} + \Sigma_{\text{fib}})$, where Σ_{fib} is the surface mass density calculated in Sect. 5.2. The gas mass fraction is plotted as a function of M_{\star} in the left hand panel of Fig. 12, where centrals are in grey and satellites in black. Solid lines represent the median μ_{gas} in bins of stellar mass, while the dashed lines indicate the the 16th and 84th percentiles. The gas mass fraction decreases as galaxies become progressively more massive, and no significant difference is seen between centrals and satellites. We also determined the 16th, 50th and 84th percentiles of the gas-phase metallicity of centrals and satellites in different bins of μ_{gas} , as shown in the right hand panel of Fig. 12. For both centrals and satellites, the oxygen abundance decreases with increasing gas mass fraction, in agreement with the findings of Zhang et al. (2009), Erb et al. (2006) and Erb et al. (2008, for galaxies at $z \sim 2$). However, at fixed μ_{gas} satellites are typically metal richer than centrals, by 0.06 dex at $\mu_{\text{gas}} \simeq 0.1$ to 0.12 dex at $\mu_{\text{gas}} \simeq 0.6$. This trend likely arises from the anti-correlation between μ_{gas} and M_{\star} , combined with the fact that, at fixed M_{\star} , satellites are metal richer than centrals. We conclude that the difference in gas phase metallicity between centrals and satellites is not associated with a difference in (indirectly

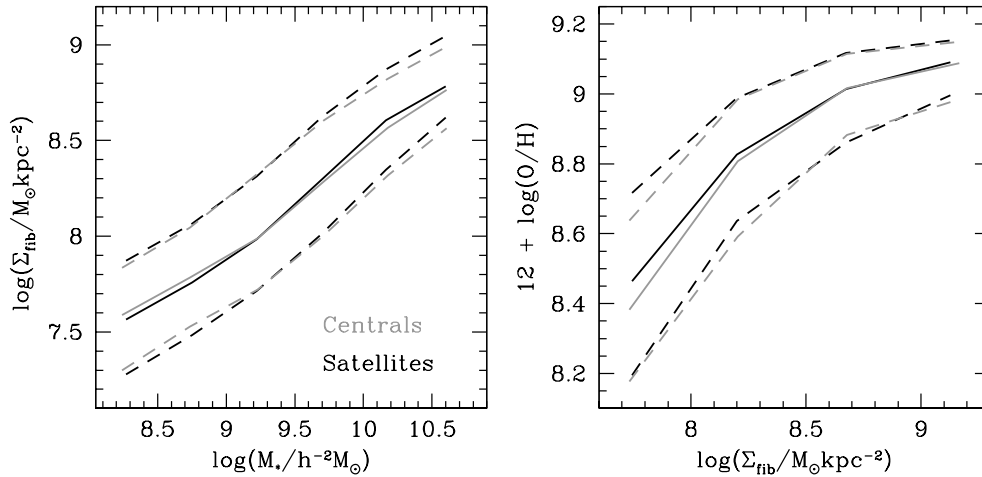


Figure 11. *Left:* the surface mass density in the fibre as a function of stellar mass for centrals (grey) and satellites (black). The solid lines show the median Σ_{fib} while the dashed lines the 16th and 84th percentiles in different bins of stellar mass. *Right:* the dependence of gas-phase metallicity on Σ_{fib} for central (grey) and satellite (black) galaxies.

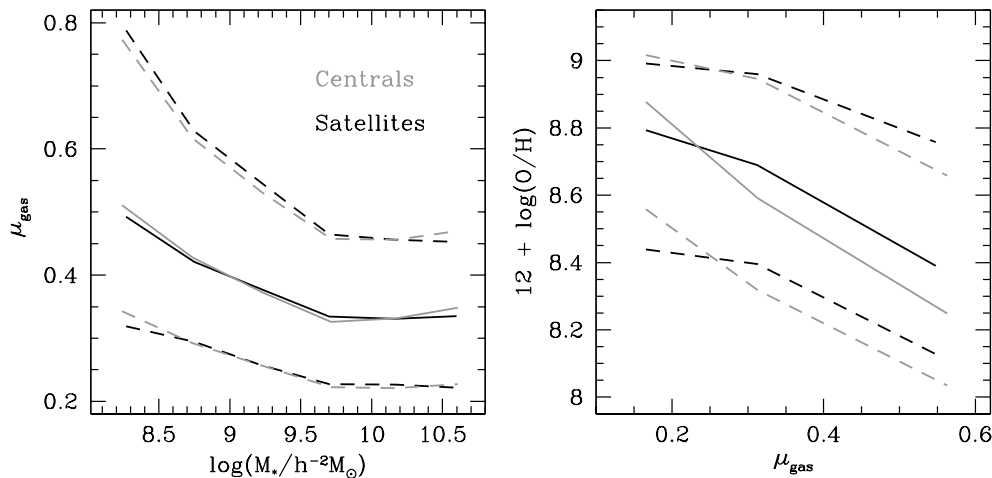


Figure 12. *Left:* the gas mass fraction in the fibre as a function of stellar mass for centrals (grey) and satellites (black). The solid lines show the median μ_{gas} while the dashed lines the 16th and 84th percentiles in different bins of stellar mass. *Right:* the dependence of gas-phase metallicity on μ_{gas} for central (grey) and satellite (black) galaxies.

inferred) gas mass fraction, as would have been expected in a simple closed box model.

5.4 Star formation rates

The results in the previous two subsections show that the enhanced gas-phase metallicities of satellite galaxies are not associated with any enhancement or suppression of the stellar surface mass density or the gas mass fractions. We now test whether there is any correlation with the star formation rates.

Fig. 13 shows the specific star formation rate in the fibre [$\text{sSFR}_{\text{fib}} = \log(\text{SFR}_{\text{fib}}/m_{\text{fib}})$] and the specific global star formation rate [$\text{sSFR}_{\text{glo}} = \log(\text{SFR}_{\text{glo}}/M_{\star})$] as a function of stellar mass for centrals (grey) and satellites (black) in sample *G*. The sSFR_{fib} of satellites is higher by only 0.02 dex than that of equally massive centrals in the range $9 < \log(M_{\star}/h^{-2}M_{\odot}) < 10.5$. The KS two sample test applied to the cumulative distributions in sSFR_{fib} of centrals and

satellites in different bins of stellar mass indicates that such a difference is not statistically significant.¹ We checked that the differences in gas-phase metallicity between satellites and centrals do not disappear when galaxies are matched in sSFR_{fib} and stellar mass.

Interestingly, the median sSFR_{glo} of satellites is systematically lower than that of centrals by 0.03 dex on average at any stellar mass. The KS two sample test run on the cumulative distributions in sSFR_{glo} of centrals and satellites in different bins in M_{\star} indicates that this difference is statistically robust at $>95\%$ confidence level, at any stellar mass. The fact that satellites have lower global star formation rates than centrals of the same stellar mass is consistent with numerous other studies (e.g., Weinmann et al. 2006, 2009; Kimm et al. 2007; Cooper et al. 2007; van den Bosch et al. 2008a,b; Pasquali et al. 2010; Peng et al. 2010; Wetzel,

¹ The same result is obtained when central and satellite galaxies are compared in their sSFR_{fib} defined as $\log(\text{SFR}_{\text{fib}}/M_{\star})$.

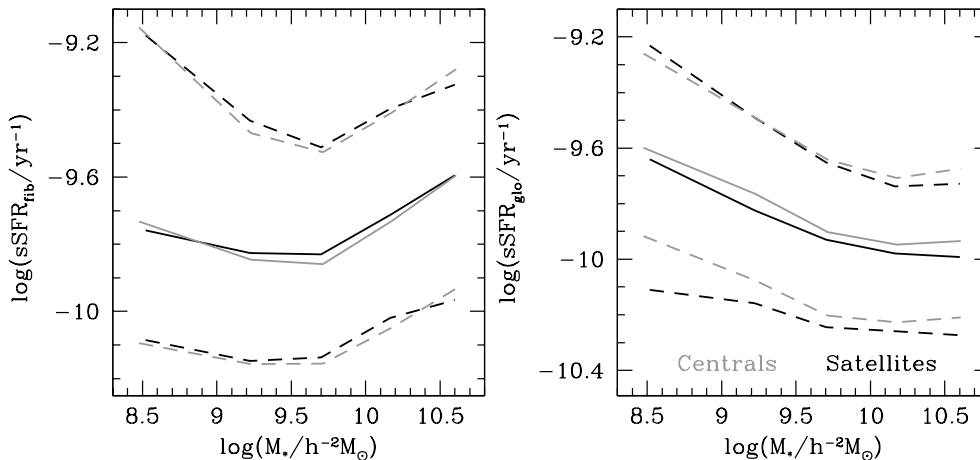


Figure 13. The dependence of the specific star formation rate in the fibre (sSFR_{fib}) and the specific global star formation rate (sSFR_{glo}) as a function of stellar mass for centrals (grey) and satellites (black) in sample *G*. The solid lines indicate the median specific SFR and the dashed lines the 16th and 84th percentiles of the distribution in specific SFR in different bins of stellar mass.

Tinker & Conroy 2011), and indicates that certain processes operating on satellite galaxies causes them to quench their star formation. The fact that our results indicate that satellites have lower sSFR_{glo} than centrals, but are equally active in their central regions (within the fibre), suggests that this quenching is an outside-in process.

5.5 Beyond a closed box

The results in the previous subsections have shown that the differences in gas-phase metallicities between centrals and satellites cannot be understood within a simple closed-box model for their chemical evolution. This should not come as a surprise, since galaxies are not expected to be closed boxes. Rather they experience inflows, outflows and even mass stripping. Interestingly, the efficiency of these processes is expected to depend strongly on environment, which, as we argue below, has the potential of explaining the trends identified in this paper.

5.5.1 Strangulation

Central galaxies that reside in host haloes with $M_{\text{h}} \lesssim 10^{12} h^{-1} M_{\odot}$ are expected to accrete cold gas from their surroundings (‘cold flows’), whereas centrals in more massive haloes are expected to accrete most of their gas through cooling flows from their hot gaseous haloes (e.g., Birnboim & Dekel 2003; Kereš et al. 2005). Satellite galaxies, however, are likely to be ‘deprived’ of these inflows, simply because their gas reservoir, be it hot or cold, is likely to be stripped by tidal forces and/or ram-pressure from the hot gaseous atmosphere associated with the host halo. Since inflows are likely to be metal-poor, this ‘strangulation’ (Larson et al. 1980) of satellite galaxies is expected to suppress the dilution of their ISM, resulting in gas-phase metallicities that are higher than those of central galaxies, in qualitative agreement with the data. Furthermore, as already discussed in Pasquali et al. (2010), present-day satellites in more massive haloes were, on average, accreted earlier (see also De Lucia et al. 2012). Hence, satellites in more massive haloes have been ‘deprived of dilution’ for a

longer time than satellites of the same stellar mass in less massive haloes, which might explain why the gas-phase metallicity of satellites increases with host halo mass (see Fig. 7), at least qualitatively.

However, strangulation is unlikely to be the entire picture. First of all, if the differences in gas-phase metallicity (within the fibre) are due to differences in the amount of dilution, this should probably show up as differences in the gas mass fraction (again within the fibre). As is evident from Fig. 12, such difference is absent, although we caution that these ‘gas mass fractions’ are indirectly inferred from the star formation rates (within the fibre). We conclude that strangulation is likely to play a role in regulating the gas-phase metallicities of satellite galaxies, but that direct data on the gas mass fractions of satellite galaxies, combined with detailed hydrodynamical simulations of strangulation, are needed to test whether strangulation in itself can explain the various trends presented in this paper.

5.5.2 Ram-Pressure Stripping and Galaxy Harassment

In addition to strangulation, there are two other mechanisms that may impact gas-phase metallicities and which operate on satellites but not on centrals: ram-pressure stripping (e.g., Gunn & Gott 1972) and galaxy harassment (e.g., Farouki & Shapiro 1981; Moore et al. 1996). We now discuss how these two processes may cause satellite galaxies to have higher gas-phase metallicities than centrals of the same stellar mass.

An important mechanism for regulating the gas-phase metallicities of (the inner regions of) disk galaxies is radial gas flows. Angular momentum redistribution within the disk, due to torques from bars, spirals and/or interacting galaxies can cause the cold gas at large galactocentric radii to move inwards (cf. Roškar et al. 2008; Minchev et al. 2012). Since galaxies typically have metallicity gradients that decline outwards, such radial gas flows will dilute the gas in the inner regions. Since satellite galaxies are exposed to stronger tidal forces, and to high-speed impulsive encounters (i.e., galaxy harassment), they are more likely to experience such diluting radial flows than central galaxies. If this were an

important mechanism, satellite galaxies would have central gas-phase metallicities that are lower than central galaxies, opposite to what is observed. This suggests that, contrary to what we postulated above, satellite galaxies do *not* experience (an enhancement in) radial gas flows. This could come about if ram-pressure and/or tidal forces strip the outer, metal-poor gas before it has the opportunity to migrate inwards. In that case, satellite galaxies are less likely to experience diluting, radial gas flows than centrals, which again might explain why the latter have lower gas-phase metallicities than the former (see also Shields, Skillman & Kennicutt (1991) and Petropoulou et al. (2011)).

There is ample observational evidence to support the notion that ram-pressure stripping is an important mechanism, at least in cluster environments (e.g., Gavazzi et al. 2001; Solanes et al. 2001; Koopmann & Kenney 2004; Abramson et al. 2011). This is also supported by detailed hydrodynamical simulations (e.g., Abadi et al. 1999; Roediger & Hensler 2005; Kronberger et al. 2008; Bekki 2009). However, the overall efficiency of ram-pressure stripping (i.e., what fraction of the gas is stripped and on what time scale) is still a matter of debate, mainly because the simulations have shown that it is a strong function of the porosity of the galaxy’s ISM (e.g., Quilis et al. 2000; Tonnesen & Bryan 2009). What is well established, though, is that ram-pressure stripping is more efficient for less massive galaxies in more massive environments (e.g., Gunn & Gott 1972; Bekki 2009). This makes the simple prediction that the suppression of metallicity-dilution in satellite galaxies increases with decreasing stellar mass and with increasing host halo mass; this is consistent with the observed trends, at least qualitatively. Another effect that may contribute here is again the distribution of infall times; since low mass satellites are typically accreted earlier than their massive counterparts (e.g., De Lucia et al. 2012), they have been exposed to the ‘corrosion’ exerted by their environments for a longer period. If ram-pressure stripping indeed causes satellite galaxies to have gas-phase metallicities that are higher (i.e., less diluted) than those of centrals of the same stellar mass, then the statistics of infall times would contribute to explaining the observed trends of gas-phase metallicities of satellites as a function of M_* and M_h .

An interesting consequence of ram-pressure stripping, which may have important consequences for our discussion, is that the gas that is not stripped away, which is mainly the gas at small galactocentric radii, may actually be compressed by the ram-pressure, giving rise to (significantly) enhanced star formation in the disk (e.g., Dressler & Gunn 1983; Gavazzi et al. 1995; Kronberger et al. 2008; Kapferer et al. 2009). Our results that satellite galaxies have the same SFRs in their central regions (within the fibre) as centrals of the same stellar mass (see Fig. 13), therefore seems to argue that ram-pressure stripping is not very efficient. On the other hand, there are clear indications that the *global* SFRs of satellites are suppressed with respect to those of centrals, which might be an indication that ram-pressure stripping has started to remove gas from the outer disks. A ram-pressure stripping induced boost in the SFR will also lead to an increase in the amount of metals returned to the ISM. However, whether these metals can be retained or whether they are ejected and/or stripped is likely to depend on many factors, to the extent that it is unclear whether

this boost in SFR is expected to increase or decrease the gas-phase metallicities. More detailed studies, in particular of the HI content of satellites versus centrals, will be needed to investigate the potential impact of ram-pressure stripping for explaining the gas-phase metallicities of satellite galaxies.

5.5.3 Galactic Wind Confinement

Another environment-dependent process that may potentially play a role in ‘regulating’ the gas phase metallicities of satellite galaxies is galactic wind confinement. When a galaxy, central or satellite, is located within a dark matter halo that has a hot gaseous atmosphere, the associated pressure may be able to inhibit a potential supernova-driven galactic wind from escaping the galaxy. Since galactic winds are typically metal-enhanced (e.g., Mac-Low & Ferrara 1999; Dalcanton 2007), systems in which the winds can escape are expected to have lower gas-phase metallicities than systems in which the wind material is confined to be recycled within the ISM of the galaxy itself. Since satellite galaxies reside in more massive host haloes than central galaxies of the same stellar mass, galactic wind confinement might explain why the former have higher oxygen abundances than the latter.

This mechanism also nicely explains the observed trends with both stellar mass and halo mass, at least qualitatively. After all, the hot gaseous atmosphere in more massive haloes has higher pressure, and is therefore better able to confine winds. This might explain why the difference in gas-phase metallicities between centrals and satellites is larger for satellites in more massive host haloes. In addition, since winds are expected to be more efficient in less massive haloes, which host less massive centrals, the potential impact of winds is more important for less massive galaxies, providing a qualitative explanation for the scalings with stellar mass. The recent simulations developed by Bahé et al. (2012) indicate that ram pressure is larger than the confinement pressure independently of halo mass. Only a small fraction of the simulated galaxies ($\sim 16\%$) appears to be confinement dominated, but this occurs when they have already gone through the first pericentre passage, where ram pressure is highest, and have hence lost most of their hot gas.

6 CONCLUSIONS

We used the groups catalogue of Yang et al. (2007) together with the DR4 catalogue of stellar ages and metallicities of Gallazzi et al. (2005), the DR4 compilation of gas-phase metallicities of Tremonti et al. (2004) and the DR7 catalogue of star formation rates of Brinchmann et al. (2004), to study the gas-phase metallicity of central and satellite galaxies and its dependence on their stellar mass and the dark matter mass of their host environments. We find that:

- i)* satellites have on average higher gas-phase metallicities than central galaxies of the same M_* . The magnitude of this differences depends on stellar mass, increasing from 0.004 dex at $\log(M_*/h^{-2}M_\odot) \simeq 10.75$ to 0.06 dex at $\log(M_*/h^{-2}M_\odot) \simeq 8.25$.
- ii)* Within the same host halo, satellites have lower gas-phase metallicities than their central galaxies by ~ 0.5 dex on average. This simply reflects that, by definition, central

galaxies are the most massive galaxies in their halos, combined with the fact that gas-phase metallicity increases with stellar mass.

iii) At fixed M_* , the gas-phase metallicity of satellites increases with halo mass; this trend is more pronounced for less massive galaxies. Low mass satellites with $10^{8.5}h^{-2}M_\odot \leq M_* \leq 10^9h^{-2}M_\odot$ have average oxygen abundances that increase by ~ 0.15 dex between $M_h = 10^{11}h^{-1}M_\odot$ and $M_h = 10^{14}h^{-1}M_\odot$.

iv) Satellite galaxies have higher gas-phase metallicities than central galaxies with the same stellar metallicities. The magnitude of this difference increases with decreasing metallicity.

We have contrasted the gas-phase metallicities of centrals and satellites with other galaxy properties, such as stellar age, surface mass density, gas mass fraction and specific star formation rate, in order to identify the mechanism(s) responsible for the observational results listed above. Based on these comparisons we draw the following conclusions:

- Star-forming centrals and satellites have very similar stellar metallicities at fixed M_* . This basically rules out that the difference in gas-phase metallicities between centrals and satellites of the same stellar mass is a consequence of stellar mass stripping. Interestingly, this mechanism was used by Pasquali et al (2010) in order to explain a similar difference between centrals and satellites but in *stellar* metallicity for mostly quiescent galaxies. The fact that this same mechanism cannot explain the gas-phase metallicities is also immediately evident from the fact that satellites have higher gas-phase metallicities than centrals *of the same stellar metallicity* (see Fig. 10). Rather, these results suggest that the differences in $12 + \log(\text{O}/\text{H})$ have their origin in something that is specific to the gas.

- Star forming satellites and centrals show very similar surface mass densities and gas mass fractions (both measured within the fibre) at fixed M_* . Consequently, their observed offset in gas-phase metallicity remains the same when they are matched in surface mass density or gas mass fraction, rather than stellar mass. Since these quantities are an indicator of the galaxy's past, integrated star formation history (SFH) within the fibre we conclude that the differences in $12 + \log(\text{O}/\text{H})$ between centrals and satellites (which are also measured within the fibre) are not a consequence of centrals and satellites having experienced different closed-box star formation histories. Rather, we argue that the mechanism(s) responsible for this offset must be associated with differences in their inflow and/or outflow histories.

- Despite their difference in gas-phase metallicities, centrals and satellites of the same stellar mass have present-day star formation rates, measured within the fibre, that are indistinguishable. However, when corrections are made to include the star formation occurring on larger scales, outside the fibre, we find that satellites have slightly reduced global SFRs compared to centrals of the same M_* . In addition, we find that star forming satellite galaxies are characterized by somewhat older stellar ages than equally massive star forming centrals. These results suggest that the satellite galaxies have started an outside-in process of star formation quenching. We emphasize that the overall impact of quenching is small in our sample, which is a consequence of the fact that our sample is biased towards star forming galaxies, for which

gas-phase metallicities can be measured from their emission lines.

We argue that there are three mechanisms that operate on satellite galaxies and that can potentially explain why they have gas-phase metallicities that are higher than those of central galaxies of the same stellar mass: (i) strangulation, which inhibits the inflow of metal-poor gas, (ii) ram-pressure stripping of the outer, metal-poor gas-disk, thereby preventing dilution of the central gas due to radial gas flows promoted by torques, and (iii) pressure confinement of metal-enriched outflows. As we have discussed in the text, each of these three mechanisms naturally explains why the difference in gas-phase metallicity between centrals and satellites increases with decreasing stellar mass and with increasing host halo mass, at least qualitatively. More work needs to be done in order to quantitatively discriminate between these environmental processes. For example, detailed simulations of ram pressure stripping and galactic wind confinement, which include also star formation and stellar/AGN feedback, are required in order to predict the effect of these mechanisms on the observed stellar and gas-phase metallicities of satellites. From an observational point of view, determining the star formation history of satellites of different stellar mass and in different environments will constrain the time-scale over which strangulation/ram pressure stripping quench star formation, while a direct measurement of the (central and total) gas mass of satellites will test the efficiency of strangulation and ram pressure stripping.

ACKNOWLEDGMENTS

We would like to thank Christy Tremonti for helpful discussions.

Funding for the SDSS and SDSS-II has been provided by the Alfred P. Sloan Foundation, the Participating Institutions, the National Science Foundation, the U.S. Department of Energy, the National Aeronautics and Space Administration, the Japanese Monbukagakusho, the Max Planck Society, and the Higher Education Funding Council for England. The SDSS Web Site is <http://www.sdss.org/>. The SDSS is managed by the Astrophysical Research Consortium for the Participating Institutions. The Participating Institutions are the American Museum of Natural History, Astrophysical Institute Potsdam, University of Basel, University of Cambridge, Case Western Reserve University, University of Chicago, Drexel University, Fermilab, the Institute for Advanced Study, the Japan Participation Group, Johns Hopkins University, the Joint Institute for Nuclear Astrophysics, the Kavli Institute for Particle Astrophysics and Cosmology, the Korean Scientist Group, the Chinese Academy of Sciences (LAMOST), Los Alamos National Laboratory, the Max-Planck-Institute for Astronomy (MPIA), the Max-Planck-Institute for Astrophysics (MPA), New Mexico State University, Ohio State University, University of Pittsburgh, University of Portsmouth, Princeton University, the United States Naval Observatory, and the University of Washington.

REFERENCES

- Abadi, M.G., Moore, B., Bower, R.G., 1999, *MNRAS*, 308, 947
- Abramson, A., Kenney, J.D.P., Crawl, H.H., Chung, A., van Gorkom, J.H., Vollmer, B., Schiminovich, D., 2011, *AJ*, 141, 164
- Adelman-McCarthy, J.K. et al., 2006, *ApJS*, 162, 38
- Bahé, Y.M., McCarthy, I.G., Crain, R.A., Theuns, T., 2012, accepted by *MNRAS* (arXiv:1205.2549)
- Bell, E.F., McIntosh, D.H., Katz, N., Weinberg, M.D., 2003, *ApJS*, 149, 289
- Bekki, K., 2009, *MNRAS*, 399, 2221
- Bekki, K., Couch, W.J., Shioya, Y., 2002, *ApJ*, 577, 651
- Birnboim, Y., Dekel, A., 2003, *MNRAS*, 345, 349
- Blanton, M.R. et al., 2003, *ApJ*, 594, 186
- Blanton, M.R. et al., 2005, *AJ*, 129, 2562
- Brinchmann, J., Charlot, S., White, S.D.M., Tremonti, C., Kauffmann, G., Heckman, T., Brinkmann, J., 2004, *MNRAS*, 351, 1151
- Brooks, A.M., Governato, F., Booth, C.M., Willman, B., Gardner, J., Wadsley, J., Stinson, G., Quinn, T., 2007, *ApJ*, 655, L17
- Bruzual, G., Charlot, S., 2003, *MNRAS*, 344, 1000
- Calura, F., Pipino, A., Chiappini, C., Matteucci, F., Maiolino, R., 2009, *A&A*, 504, 373
- Chabrier, G., 2003, *PASP*, 115, 763
- Charlot, S., Fall, S.M., 2000, *ApJ*, 539, 718
- Charlot, S., Longhetti, M., 2001, *MNRAS*, 323, 887
- Cooper, M.C., et al., 2007, *MNRAS*, 376, 1445
- Cooper, M.C., Tremonti, C.A., Newman, J.A., Zabludoff, A.I., 2008, *MNRAS*, 390, 245
- Crawl, H.H., Kenney, J.D.P., Chung, A., Blanton, M., van Gorkom, J.H., 2010, *ASP Conf. Ser.*, 423, 97
- Dalcanton, J.J., 2007, *ApJ*, 658, 941
- Davé, R., Finlator, K., Oppenheimer, B.D., Fardal, M., Katz, N., Kereš, D., Weinberg, D.H., 2010, *MNRAS*, 404, 1355
- De Lucia, G., Weinmann, S., Poggianti, B.M., Aragón-Salamanca, A., Zartsky, D., 2012, *MNRAS*, submitted
- Dressler, A., Gunn, J.E., 1983, *ApJ*, 270, 7
- Edmunds, M.G., 1990, *MNRAS*, 246, 678
- Ellison, S.L., Patton, D.R., Simard, L., McConnachie, A.W., 2008, *AJ*, 135, 1877
- Ellison, S.L., Simard, L., Cowan, N.B., Baldry, I.K., Patton, D.R., McConnachie, A.W., 2009, *MNRAS*, 396, 1257
- Erb, D.K., 2008, *ApJ*, 674, 151
- Erb, D.K., Shapley, A.E., Pettini, M., Steidel, C.C., Reddy, N.A., Adelberger, K.L., 2006, *ApJ*, 644, 813
- Farouki, R.T., Shapiro, S.L., 1982, *ApJ*, 259, 103
- Ferland, G., 1996, *Hazy: A Brief Introduction to CLOUDY*. Internal Report, Univ. Kentucky
- Finlator, K., Davé, R., 2008, *MNRAS*, 385, 2181
- Frye, B., Broadhurst, T., Benítez, N., 2002, *ApJ*, 568, 558
- Gallazzi, A., Charlot, S., Brinchmann, J., White, S.D.M., Tremonti, C.A., 2005, *MNRAS*, 362, 41
- Garnett, D.R., 2002, *ApJ*, 581, 1019
- Garnett, D.R., Shields, G.A., 1987, *ApJ*, 317, 82
- Gavazzi, G., Contursi, A., Carrasco, L., Boselli, A., Kennicutt, R., Scodreggio, M., Jaffe, W., 1995, *A&A*, 304, 325
- Gavazzi, G., Boselli, A., Mayer, L., Iglesias-Paramo, J., Vilchez, J.M., Carrasco, L., 2001, *ApJ*, 563, L23
- Gavazzi, G., Boselli, A., Pedotti, P., Gallazzi, A., Carrasco, L., 2002, *A&A*, 396, 449
- Gunn, J.E., Gott III, J.R., 1972, *ApJ*, 176, 1
- Kang, X., van den Bosch, F.C., 2008, *ApJ*, 676, L101
- Kapferer, W., Sluka, C., Schindler, S., Ferrari, C., Ziegler, B., 2009, *A&A*, 499, 87
- Kauffmann, G. et al., 2003, *MNRAS*, 341, 54
- Kennicutt, R.C., Jr., 1998, *ApJ*, 498, 541
- Kereš, D., Katz, N., Weinberg, D.H., Davé, R., 2005, *MNRAS*, 363, 2
- Kimm, T. et al., 2009, *MNRAS*, 394, 1131
- Kobayashi, C., Springel, V., White, S.D.M., 2007, *MNRAS*, 376, 1465
- Koopmann, R.A., Kenney, J.D.P., 2004, *ApJ*, 613, 866
- Köppen, J., Weidner, C., Kroupa, P., 2007, *MNRAS*, 375, 673
- Kronberger, T., Kapferer, W., Ferrari, C., Unterguggenberger, S., Schindler, S., 2008, *A&A*, 481, 337
- Lara-López, M.A. et al., 2010, *A&A*, 521, L53
- Larson, R.B., Tinsley B.M., Caldwell C.N., 1980, *ApJ*, 237, 692
- Lee, H., McCall, M.L., Richer, M.G., 2003, *AJ*, 125, 2975
- Lehnert, M.D., Heckman, T.M., 1996, *ApJ*, 462, 651
- Lequeux, J., Peimbert, M., Rayo, J.F., Serrano, A., Torres-Peimbert, S., 1979, *A&A*, 80, 155
- Mahajan, S., Haines, C.P., Raychaudhury, S., 2010, *MNRAS*, 404, 1745
- Mannucci, F., Cresci, G., Maiolino, R., Marconi, A., Gnerucci, A., 2010, *MNRAS*, 408, 2115
- McCarthy, I.G., Schaye, J., Bower, R.G., Ponman, T.J., Booth, C.M., Dalla Vecchia, C., Springel, V., 2011, *MNRAS*, 412, 1965
- Minchev, I., Famaey, B., Quillen, A.C., Di Matteo, P., Combes, F., Vlahic, M., Erwin, P., Bland-Harworthorn, J., 2012, *A&A*, submitted (arXiv:1203.2621)
- Moore, B., Katz, N., Lake, G., Dressler, A., Oemler, A., 1996, *Nature*, 379, 613
- More, S., van den Bosch, F.C., Cacciato, M., Skibba, R., Mo, H.J., Yang, X., 2011, *MNRAS*, 410, 210
- Mouhcine, M., Baldry, I.K., Bamford, S.P., 2007, *MNRAS*, 382, 801
- Mouhcine, M., Gibson, B.K., Renda, A., Kawata, D., 2008, arXiv:0801.2476
- Muldrew, S.I. et al., 2012, *MNRAS*, 419, 2670
- Pasquali, A., Gallazzi, A., Fontanot, F., van den Bosch, F.C., De Lucia, G., Mo, H.J., Yang, X., 2010, *MNRAS*, 407, 937
- Pasquali, A., van den Bosch, F.C., Mo, H.J., Yang, X., Somerville, R., 2009, *MNRAS*, 394, 38
- Peeples, M.S., Shankar, F., 2011, *MNRAS*, 417, 2962
- Peng, Y., et al. 2010, *ApJ*, 721, 193
- Petropoulou, V., Vílchez, J., Iglesias-Páramo, J., Papaderos, P., Magrini, L., Cedrés, B., Reverte, D., 2011, *ApJ*, 734, 32
- Petrosian, V., 1976, *ApJ*, 209, L1
- Pustilnik, S.A., Tepliakova, A.L., Kniazev, A.Y., 2011, *MNRAS*, 417, 1335
- Quilis, V., Moore, B., Bower, R.G., 2000, *Science*, 288, 1617
- Roediger, E., Hensler, G., 2005, *A&A*, 433, 875
- Roškar, R., Debattista, V.P., Stinson, G.S., Quinn, T.R., Kaufmann, T., Wadsley, J., 2008, *ApJ*, 675, 65
- Salim, S. et al., 2005, *ApJ*, 619, L39

- Salim, S. et al., 2007, *ApJS*, 173, 267
- Scannapieco, C., Tissera, P.B., White, S.D.M., Sringel, V., 2008, *MNRAS*, 389, 1137
- Shields, G.A., Skillman, E.D., Kennicutt, R.C., 1991, *ApJ*, 371, 82
- Schlegel, D.J., Finkbeiner, D.P., Davis, M., 1998, *ApJ*, 500, 525
- Skillman, E.D., Kennicutt, R.C., Hodge, P.W., 1989, *ApJ*, 347, 875
- Skillman, E.D., Kennicutt, R.C., Shields, G.A., Zaritsky, D., 1996, *ApJ*, 462, 147
- Solanes, J.M., Manrique, A., García-Gómez, C., González-Casado, G., Giovanelli, R., Haynes, M.P., 2001, *ApJ*, 548, 97
- Spergel, D.N. et al., 2007, *ApJS*, 170, 377
- Spitoni, E., Calura, F., Matteucci, F., Recchi, S., 2010, *A&A*, 514, A73
- Strateva, I. et al., 2001, *AJ*, 122, 1861
- Strauss, M.A. et al., 2002, *AJ*, 124, 1810
- Tonnesen, S., Bryan, G.L., 2009, *ApJ*, 694, 789
- Tremonti, C. et al., 2004, *ApJ*, 613, 898
- van den Bosch, F.C., Aquino, D., Yang, X., Mo, H.J., Pasquali, A., McIntosh, D.H., Weinmann, S.M., Kang, X., 2008a, *MNRAS*, 387, 79
- van den Bosch, F.C., Pasquali, A., Yang, X., Mo, H.J., Weinmann, S., McIntosh, D.H., Aquino, D., 2008b, *arXiv:0805.0002*
- Vílchez, J.M., 1995, *AJ*, 110, 1090
- Weinmann, S.M., van den Bosch, F.C., Yang, X., Mo, H.J., 2006, *MNRAS*, 366, 2
- Weinmann, S.M., Kauffmann, G., van den Bosch, F.C., Pasquali, A., McIntosh, D.H., Mo, H., Yang, X., Guo, Y., 2009, *MNRAS*, 394, 1213
- Weiner, B.J. et al., 2009, *ApJ*, 692, 187
- Wetzell, A., Tinker, J., Conroy, C., 2011, submitted to *MNRAS* (*arXiv:1107.5311*)
- Yang, X., Mo, H.J., van den Bosch, F.C., Jing, Y.P., 2005, *MNRAS*, 356, 1293
- Yang, X., Mo, H.J., van den Bosch, F.C., Pasquali, A., Li, C., Barden, M., 2007, *ApJ*, 671, 153
- Yang, X., Mo, H.J., van den Bosch, F.C., 2008, *ApJ*, 676, 248
- Yates, R.M., Kauffmann, G., Guo, Q., 2012, *MNRAS*, 422, 215
- Zaritsky, D., Kennicutt, R.C., Huchra, J.P., 1994, *ApJ*, 420, 87
- Zehavi, I. et al., 2002, *ApJ*, 571, 172
- Zhang, W., Li, C., Kauffmann, G., Zou, H., Catinella, B., Shen, S., Guo, Q., Chang, R., 2009, *MNRAS*, 397, 1243